

Published in final edited form as:

Metallomics. 2013 March 27; 5(3): 208–213. doi:10.1039/c3mt20158a.

Zinc released from olfactory bulb glomeruli by patterned electrical stimulation of the olfactory nerve

Laura J. Blakemore^{a,b}, Elisa Tomat^c, Stephen J. Lippard^c, and Paul Q. Trombley^{a,b,*}

^aDepartment of Biological Science, The Florida State University, Tallahassee, FL 32306

^bProgram in Neuroscience, The Florida State University, Tallahassee, FL 32306

^cDepartment of Chemistry, Massachusetts Institute of Technology, Cambridge, MA 02139

Abstract

Zinc is a trace element with a multitude of roles in biological systems including structural and cofactor functions for proteins. Although most zinc in the central nervous system (CNS) is protein bound, the CNS contains a pool of mobile zinc housed in synaptic vesicles within a subset of neurons. Such mobile zinc occurs in many brain regions, such as the hippocampus, hypothalamus, and cortex, but the olfactory bulb (OB) contains one of the highest such concentrations in the CNS. Zinc is distributed throughout the OB, with the glomerular and granule cell layers containing the highest levels. Here, we visualize vesicular zinc in the OB using zinc-responsive fluorescent probes developed by one of us. Moreover, we provide the first demonstration that vesicular pools of zinc can be released from olfactory nerve terminals within individual glomeruli by patterned electrical stimulation of the olfactory nerve designed to mimic the breathing cycle in rats. We also provide electrophysiological evidence that elevated extracellular zinc potentiates α -amino-3-hydroxy-5-methyl-4-isoxazolepropionic acid (AMPA) receptor-mediated synaptic events. AMPA receptors are required for the synchronous activation of neurons within individual OB glomeruli, and zinc-mediated potentiation leads to enhanced synaptic summation.

Introduction

Zinc within synaptic vesicles in the central nervous system (CNS) is colocalized mostly with glutamate in a subset of glutamatergic “zinc-enriched” neurons^{1–6}. This finding, combined with evidence that depolarizing stimuli can release vesicular zinc, supports the view that zinc is released during synaptic transmission^{7–10}. Although the exact quantity released is unknown, resulting extracellular zinc concentrations have been proposed to range from 10–300 μ M^{8–12}.

Most studies on synaptically released zinc have focused on the mossy fiber/CA3 pathway in the hippocampus. It has just been reported that vesicular zinc is required for presynaptic mossy fiber-long term potentiation and also inhibits a form of postsynaptic mossy fiber-long term potentiation¹³. A full understanding of the role of this pathway will require more work, in part due to the complexity of the circuitry of the hippocampus. In contrast, in the olfactory system, olfactory sensory neurons (OSNs) in the nose project their axons, via the first cranial nerve, into the olfactory bulb (OB), the first region of the brain involved in odor information processing. In the OB, OSN axon terminals make contact with OB neurons in discrete anatomical structures called glomeruli. OSN nerve terminals in these glomeruli

*Corresponding author. 207 Biomedical Research Facility, Department of Biological Science, Florida State University, Tallahassee, FL 32306-4340. Tel: 850-644-1614; fax: 850-644-0989; trombley@neuro.fsu.edu..

contain a high concentration of vesicular zinc. Because the function of this pathway is well defined, namely to transmit olfactory sensory information to the brain, the OB lacks the complexity of the hippocampus and is an ideal model system to explore the function of synaptically released zinc.

Results from a variety of other studies provide further evidence that zinc modulates synaptic transmission. For example, zinc inhibits NMDA receptor-, kainate receptor- and GABA receptor-mediated responses in the hippocampus^{14–19}, and we have reported similar findings in OB neurons^{20–22}. We have also shown that zinc has complex concentration-dependent, biphasic (potentiation/inhibition) effects on native OB AMPA receptors (AMPA) that appear to depend on the molecular composition of the receptor²³. Additional effects of zinc on neuronal excitability within the OB include modulation of several types of voltage-gated ion channels²⁰. Collectively, these results support the notion that synaptically released zinc influences synaptic transmission and neuronal excitability via multiple mechanisms. In the present study, we use the zinc-sensitive fluorescent probe Zinpyr-1 (ZP1)²⁴ to test the hypothesis that patterned stimuli can evoke the release of zinc from OSN nerve terminals. We also demonstrate that elevated extracellular zinc levels potentiate AMPAR-mediated synaptic events resulting in synaptic summation.

Materials and Methods

Animal Use

The animals used for these experiments were used according to the guidelines of our protocol approved by Florida State University's Animal Care and Use Committee and the National Institutes of Health Guide for the Care and Use of Laboratory Animals (NIH Publications No. 80-23).

Preparation of olfactory bulb slices for imaging

Olfactory bulb slices were prepared from 16–21-day-old Sprague Dawley rats that were anesthetized with halothane and then killed by decapitation. Bulbs were rapidly removed and placed in ice-cold oxygenated (95% O₂ and 5% CO₂) saline solution containing (in mM): 83 NaCl, 26.2 NaHCO₃, 2.5 KCl, 1 NaH₂PO₄, 3.3 MgCl₂, 0.5 CaCl₂, 22 glucose, and 72 sucrose. Horizontal slices (400 μm) were made with a Vibratome and incubated in a holding chamber for 30 min at 35°C in a saline solution containing (in mM): 125 NaCl, 25 NaHCO₃, 1.25 NaH₂PO₄, 25 glucose, 2.5 KCl, 1.0 MgCl₂ and 2 CaCl₂, pH 7.3. Slices were then incubated in this solution at 20–24°C during the exposure to the zinc probe and chelators. ZP1 was synthesized as previously reported²⁴. For imaging, slices were placed in a recording chamber and viewed with a Leica microscope equipped with DIC optics. Electrical stimulation of olfactory sensory neuron axons was conducted with a patch pipette filled with extracellular solution. Stimulus pulses were generated by a computer running AxoGraph software (Sydney, Australia), which triggered a stimulus isolation unit (stimulations ranged from 200–500 μA).

Electrophysiology

Whole-cell current- and voltage-clamp recordings were made at room temperature from OB neurons after 7 to 21 days in primary culture as previously described²³. The recording chamber was perfused at 0.5–2.0 mL/min with a bath solution containing (in mM): NaCl, 162.5; KCl, 2.5; CaCl₂, 2; MgCl₂, 1; HEPES, 10; glucose, 10. The pH was adjusted to 7.3 with NaOH. The final osmolarity was 325 mOsm. Patch electrodes were pulled from borosilicate glass to a final electrode resistance of 4–6 MΩ. These electrodes were filled with a solution containing (in mM): KMeSO₄, 145; MgCl₂, 1; HEPES, 10; Mg-ATP, 4; Mg-GTP, 0.5; and EGTA, 1.1 (pH 7.2; osmolarity 310 mOsm).

Drugs were diluted in the bath solution and applied via a gravity-fed flow-pipe perfusion system, assembled from an array of 600 μm -I.D. square glass barrels. An electronic manipulator (Warner Instruments, Hamden, CT) was used to position the flow pipes near the neuron, and pinch clamps were used to control drug flow. This allowed neurons to be completely enveloped in a known concentration of drug and the speed of the solution changes allowed peak drug responses to occur within 100 ms. Neurons were continuously perfused with bath ("control") solution, except during drug application. Bicuculline was added to all solutions to block GABA_A receptors and isolate glutamatergic synaptic events. The applied agents were ZnCl₂ (100 μM), bicuculline (10 μM), and AP5 (100 μM) from Sigma.

Statistical analyses include Student t-test routines included in KaleidaGraph (Synergy Software, Reading, PA).

Results

To visualize the location of vesicular zinc in the OB, we used the probe Zinpyr-1 (ZP1)²⁴. ZP1 has intense visible absorption and emission spectra, and its fluorescence turn-on is selective for ionic zinc over other abundant, labile metal ions found in the CNS such as calcium or magnesium. Furthermore, ZP1 is water-soluble and membrane permeable, which allows visualization of vesicular zinc pools. Although previous investigators have reported the location of zinc in the OB, these studies used fixed tissue^{25, 26}. Because of the low toxicity of ZP1 at experimental concentrations, the data presented here advance those observations by using this probe to examine the location and release of zinc in living OB slices.

Horizontal slices from 19- to 21-day-old rats were cut at 400 μm , then incubated in 30 μM ZP1 for 30 min, and washed for 30 minutes to remove excess extracellular ZP1. Figure 1a shows the layered pattern of the organization of the OB. Both the glomerular layer (top of Fig 1a) and the granule cell layer (bottom of Fig 1a) reveal high-intensity fluorescence, reflecting ZP1 binding of zinc. Only a very weak signal was detected in the external plexiform layer, which contains very low concentrations of zinc. A higher magnification view of a glomerulus, where vesicular zinc is localized to olfactory nerve terminals, is shown in Figure 1b. A quantitative analysis of the signal intensities is shown in the insets.

To demonstrate that the signals depicted in Figure 1 reflect free ionic zinc, we applied the zinc chelator tri-2-picolylamine (TPA) at 30 μM to absorb Zn²⁺ ions from ZP1-treated slices²⁷ (Z. Huang, X-a. Zhang, and S. J. Lippard, unpublished work). Figure 2a shows a magnified view of a glomerulus after treatment with ZP1. TPA rapidly reduced the signal over a period of 10 min, demonstrating that the fluorescence emission from ZP1 reflects binding to ionic zinc (Figs 2b, 2c). Longer incubation times with TPA (>30 min) eliminated the signal from ZP1 (not shown). A quantitative analysis (n=3) of the reduction of the signal over time is shown in Figure 2d. As an additional control, we incubated ZP1-treated slices (n=3) in an extracellular solution containing 50 mM KCl. The high extracellular potassium solution eliminated the zinc signal within 10 minutes, presumably via depolarization-evoked release of zinc-containing synaptic vesicles.

Analogous observations were made when we compared the effects of TPA on the fluorescent zinc-mediated signal to that of the selective zinc chelator, *N,N,N,N*-tetrakis(2-pyridylmethyl)ethylenediamine (TPEN). OB slices were first incubated in ZP1 and then exposed to either 30 μM TPA or 30 μM TPEN for 20 min. As shown in Figure 3, both TPA and TPEN displace Zn²⁺ from the sensor and produce similar reductions in the signals.

Although several studies have provided confirmation of zinc release from the mossy fiber pathway in the hippocampus^{8–10, 13}, there have been no published reports examining zinc release in the OB. In contrast to the complex circuitry in the hippocampus, zinc-containing OSN pathways projecting to the OB are more defined. OSNs expressing the same type of odor receptor project to the same glomeruli, and odor-induced activation of these results in synchronous activation of OB neurons innervating those glomeruli.

To demonstrate release of synaptic zinc in the OB, we incubated OB slices with ZPI and used electrical stimulation of the olfactory nerve layer to evoke zinc release. The stimulating electrode was placed at the olfactory nerve-glomerular layer boundary to isolate a single, or at the most a few, glomeruli innervated by the adjacent bundle of olfactory nerve axons. To provide a natural pattern of activation, the olfactory nerve axon bundle was electrically stimulated as a pattern consisting of five bursts (three pulses at 100 Hz) separated by 250 ms (4 Hz) to mimic the breathing cycle in rats²⁸. Each stimulus pattern was applied every 10–15 s for a total duration of 10 min. As shown in Figure 4, such patterns of stimuli resulted in a selective reduction of the zinc signal in glomeruli adjacent to the stimulating electrode, while nearby glomeruli remained unchanged (n=3). Patterned stimuli reduced the zinc signal by $87.4 \pm 6.8\%$ ($p = 0.002$). A quantitative analysis of the change in the fluorescent signal is shown in Figure 4c.

To assess more directly the potential functional consequences of elevated extracellular zinc, we examined the effects of zinc on glutamate-mediated synaptic transmission in the OB using whole-cell current-clamp and voltage-clamp recordings. For these experiments, we isolated AMPA receptor-mediated excitatory post-synaptic potentials (EPSPs) in mitral cells (n=20) and interneurons (n=13). In a subset of these cells (12 mitral cells, 12 interneurons), we also examined AMPA-receptor mediated post-synaptic currents (EPSCs) in voltage-clamp mode to eliminate potential effects of zinc on voltage-activated ion channels in current-clamp mode. Consistent with our previous findings on the effects of zinc on currents evoked by exogenous AMPA application²³, we found a significant difference in the frequency of zinc-mediated potentiation between cell types that likely reflects differences in AMPA receptor subunit composition. Co-application of $100\ \mu\text{M ZnCl}_2$, $10\ \mu\text{M bicuculline}$ (to block GABA_A receptor-mediated activity), and $100\ \mu\text{M AP5}$ (to block NMDA receptor-mediated activity) potentiated AMPA receptor-mediated EPSPs and/or EPSCs in 12 of 20 (60%) of mitral/tufted (M/T) cells compared with only 3 of 13 (23%) of interneurons. Prior to zinc perfusion, M/T cell EPSP amplitude was $5.5 \pm 2.1\ \text{mV}$ versus $17.8 \pm 5.6\ \text{mV}$ after zinc perfusion (n=11; $p < 0.001$). EPSC amplitudes increased after zinc treatment from $22.5 \pm 6.0\ \text{pA}$ to $32.4 \pm 5.5\ \text{pA}$ (n=8; $p = 0.004$). Zinc perfusion reduced both EPSPs and EPSCs in a small subset of M/T cells (2 of 20) by about only 10%. In 6 of 20 M/T cells, zinc appeared to have no measureable effect. In 3 of 13 interneurons, zinc potentiated EPSCs ($13.5 \pm 2.9\ \text{pA}$ vs. $20.8 \pm 4.2\ \text{pA}$; n=3; $p < 0.05$). Among these 3 cells, EPSPs were examined in only one and this showed potentiation to about 154% of control amplitudes. Zinc-inhibited EPSPs ($9.2 \pm 3.3\ \text{mV}$ vs. $2.5 \pm 1.8\ \text{mV}$) and EPSCs ($21.3 \pm 4.1\ \text{pA}$ vs. $8.2 \pm 2.4\ \text{pA}$) in 4 of 13 interneurons ($p < 0.05$). Zinc had no measureable effect in 6 of 13 interneurons. For both cell types, the frequency of potentiation, inhibition, or no effect was similar to that observed previously with application of $100\ \mu\text{M}$ zinc during AMPA-evoked currents²³. In M/T cells, the dominant effect of zinc on AMPAR-mediated synaptic events was potentiation, and as shown in Fig 5, such potentiation contributes to summation and increases the probability of action potential generation.

Discussion

The results from the present study show, for the first time, that vesicular zinc is released from OSN terminals by patterns of electrical stimulation designed to mimic the breathing

cycle. This observation has important implications because the glomerular region of the OB expresses a high density of targets for modulation by zinc released from OSNs, including the AMPA receptors examined here. AMPA receptors in both M/T cells and juxtglomerular neurons are activated by glutamate released from OSNs. The present results extend our previous biophysical/kinetic analyses of synaptic/extrasynaptic AMPA receptors²³ by isolating the synaptically activated AMPA receptors important to OB circuit function. AMPA receptors play a key role in mediating lateral and self excitation between M/T cell apical dendrites that project to the same glomerulus^{29–31}. A subset of AMPA receptors activated by OSNs and those activated between M/T cell dendrites are calcium-permeable^{32–34}. These may be of special significance in the context of our results demonstrating synaptic release of zinc within glomeruli, as calcium-permeable AMPA receptors also flux zinc and we have recently demonstrated that elevations in intracellular zinc can modulate glycine receptors³⁵. Whether intracellular zinc can also modulate other ion channels involved in regulating neuronal excitability remains to be determined.

In many regions of the CNS, synchronization of activity is an important feature of neuronal networks. Our results demonstrate that potentiation of AMPA receptor-mediated synaptic events by zinc enhances synaptic summation and summation can contribute to synchronization. In the olfactory system, OSNs transmit information to the OB encoded by patterns of glutamate release onto OB neurons. As a result, the activity of mitral and tufted cells projecting to the same glomerulus is synchronized on both slow and fast time scales^{29, 30, 36–38} that are partially dependent on AMPA receptor activation²⁹. Such coordinated activity leads to temporal and spatial patterns of odor-evoked oscillations among OB neurons. Whereas glutamate transmission generates the initial spatial patterns, GABAergic neurons, driven by glutamatergic OB neurons (mitral and tufted cells), regulate the temporal patterns^{33, 37}. These patterns are believed to underlie the role of the OB in encoding olfactory information. AMPA receptors, and other ion channels that are targets of zinc (NMDA receptors, GABA receptors, potassium channels), all play important roles in olfactory information processing. Hence, the influence of synaptically released zinc would alter the activity of the glomerular network and the spatial and temporal patterns of network behavior underlying sensory coding by the OB.

Acknowledgments

This work was supported by grants from the US National Institutes of Health (NIH) from the National Institute of General Medical Sciences under grant GM065519 and by intramural funding from the Program in Neuroscience the Council on Research and Creativity at Florida State University.

References

1. Beaulieu C, Dyck R, Cynader M. *Neuroreport*. 1992; 3:861–864. [PubMed: 1358251]
2. Crawford IL, Connor JD. *Nature*. 1973; 244:442–443. [PubMed: 4582499]
3. Frederickson CJ. *Int Rev Neurobiol*. 1989; 31:145–238. [PubMed: 2689380]
4. Frederickson CJ, Klitenick MA, Manton WI, Kirkpatrick JB. *Brain Res*. 1983; 273:335–339. [PubMed: 6616240]
5. Haug FM. *Histochemie*. 1967; 8:355–368. [PubMed: 4876575]
6. Perez-Clausell J, Danscher G. *Brain Res*. 1985; 337:91–98. [PubMed: 2408711]
7. Aniksztejn L, Charton G, Ben-Ari Y. *Brain Res*. 1987; 404:58–64. [PubMed: 3567585]
8. Assaf SY, Chung SH. *Nature*. 1984; 308:734–736. [PubMed: 6717566]
9. Howell GA, Welch MG, Frederickson CJ. *Nature*. 1984; 308:736–738. [PubMed: 6717567]
10. Li Y, Hough CJ, Suh SW, Sarvey JM, Frederickson CJ. *J Neurophysiol*. 2001; 86:2597–2604. [PubMed: 11698545]

11. Frederickson CJ, Suh SW, Silva D, Thompson RB. *J Nutr.* 2000; 130:1471S–1483S. [PubMed: 10801962]
12. Vogt K, Mellor J, Tong G, Nicoll R. *Neuron.* 2000; 26:187–196. [PubMed: 10798403]
13. Pan E, Zhang XA, Huang Z, Krezel A, Zhao M, Tinberg CE, Lippard SJ, McNamara JO. *Neuron.* 2011; 71:1116–1126. [PubMed: 21943607]
14. Legendre P, Westbrook GL. *Mol Pharmacol.* 1991; 39:267–274. [PubMed: 1706468]
15. Mayer ML, Vyklicky L Jr. *J Physiol.* 1989; 415:351–365. [PubMed: 2561789]
16. Mott DD, Benveniste M, Dingledine RJ. *J Neurosci.* 2008; 28:1659–1671. [PubMed: 18272686]
17. Westbrook GL, Mayer ML. *Nature.* 1987; 328:640–643. [PubMed: 3039375]
18. Xie X, Gerber U, Gahwiler BH, Smart TG. *Neurosci Lett.* 1993; 159:46–50. [PubMed: 8264976]
19. Xie XM, Smart TG. *Nature.* 1991; 349:521–524. [PubMed: 1846946]
20. Horning MS, Trombley PQ. *J Neurophysiol.* 2001; 86:1652–1660. [PubMed: 11600628]
21. Trombley PQ, Horning MS, Blakemore LJ. *Neuroreport.* 1998; 9:3503–3507. [PubMed: 9855307]
22. Trombley PQ, Shepherd GM. *J Neurophysiol.* 1996; 76:2536–2546. [PubMed: 8899625]
23. Blakemore LJ, Trombley PQ. *Neuroreport.* 2004; 15:919–923. [PubMed: 15073543]
24. Burdette SC, Walkup GK, Spingler B, Tsien RY, Lippard SJ. *J Am Chem Soc.* 2001; 123:7831–7841. [PubMed: 11493056]
25. Jo SM, Won MH, Cole TB, Jensen MS, Palmiter RD, Danscher G. *Brain Res.* 2000; 865:227–236. [PubMed: 10821925]
26. Mook Jo S, Kuk Kim Y, Wang Z, Danscher G. *Brain Res.* 2002; 956:230–235. [PubMed: 12445690]
27. Ghosh SK, Kim P, Zhang XA, Yun SH, Moore A, Lippard SJ, Medarova Z. *Cancer Res.* 2010; 70:6119–6127. [PubMed: 20610630]
28. Youngentob SL, Mozell MM, Sheeche PR, Hornung DE. *Physiol Behav.* 1987; 41:59–69. [PubMed: 3685154]
29. Schoppa NE, Westbrook GL. *Nat Neurosci.* 2002; 5:1194–1202. [PubMed: 12379859]
30. Christie JM, Westbrook GL. *J Neurosci.* 2006; 26:2269–2277. [PubMed: 16495454]
31. Urban NN, Sakmann B. *J Physiol.* 2002; 542:355–367. [PubMed: 12122137]
32. Blakemore LJ, Resasco M, Mercado MA, Trombley PQ. *Am J Physiol Cell Physiol.* 2006; 290:C925–935. [PubMed: 16267106]
33. Ma J, Lowe G. *Neuroscience.* 2007; 144:1094–1108. [PubMed: 17156930]
34. Pimentel DO, Margrie TW. *J Physiol.* 2008; 586:2107–2119. [PubMed: 18276730]
35. Trombley PQ, Blakemore LJ, Hill BJ. *Neuroscience.* 2011; 186:32–38. [PubMed: 21530619]
36. Carlson GC, Shipley MT, Keller A. *J Neurosci.* 2000; 20:2011–2021. [PubMed: 10684902]
37. Schoppa NE. *Neuron.* 2006; 49:271–283. [PubMed: 16423700]
38. Schoppa NE, Westbrook GL. *Neuron.* 2001; 31:639–651. [PubMed: 11545722]

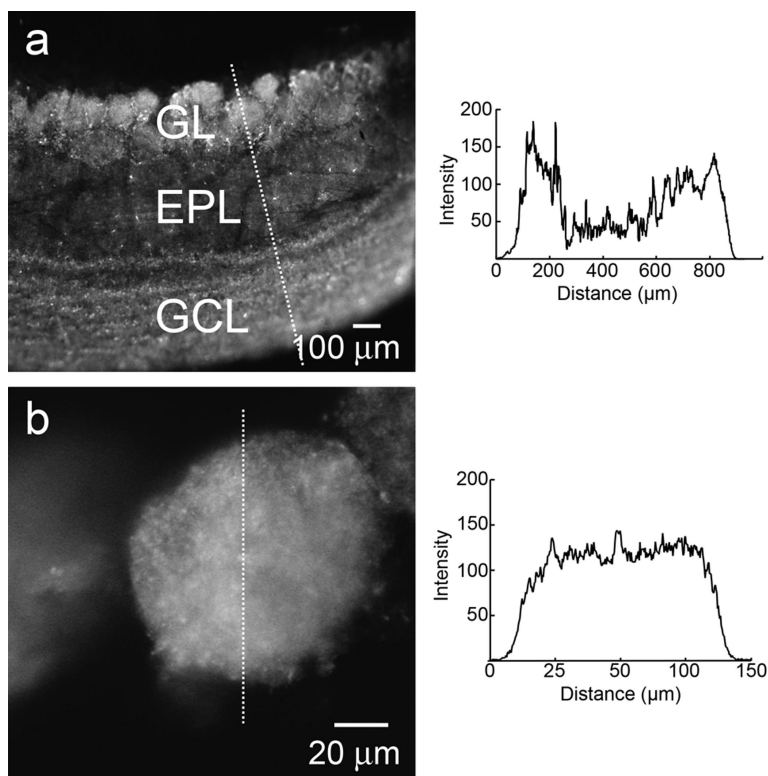


Figure 1.

Localization of vesicular zinc in the OB. Horizontal slices of the OB were cut at 400 μm and incubated in 30 μM ZP1 for 30 min. a) Intense fluorescent signals are evident within glomeruli (in the glomerular layer) and in the granule cell layer. By contrast, the external plexiform layer shows only a very weak fluorescent signal. b) A high magnification view of the glomerular layer demonstrates the intensity of the vesicular zinc signal within glomeruli. The insets show quantitative measurements of the zinc signal in the images as measured along the lines drawn across the images using the plot analysis feature in ImageJ and background subtracted. Glomerular Layer (GL); External Plexiform Layer (EPL); Granule Cell Layer (GCL).

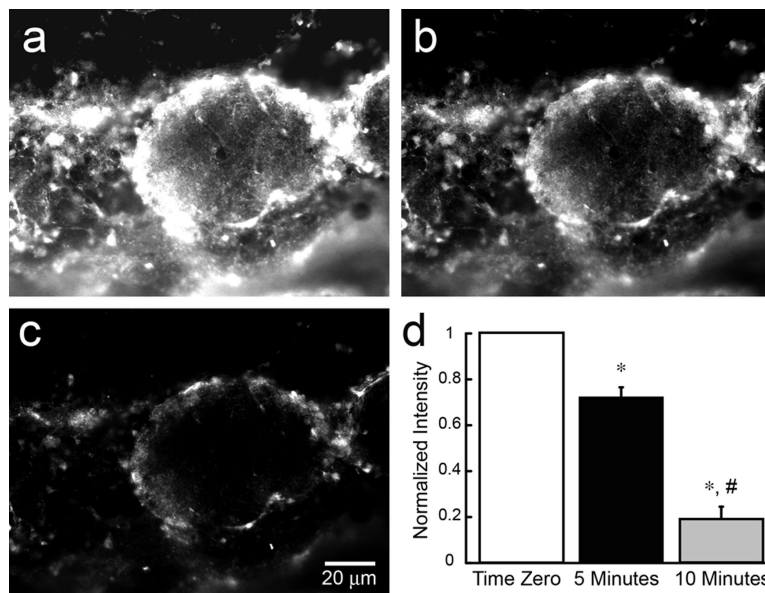


Figure 2. Chelation of zinc with TPA reduces the signal from ZP1. OB slices were incubated in 30 μ M ZP1 for 30 min after which 30 μ M of the zinc chelator, TPA, was added. The images show high magnification views of the glomerular layer. a) The signal at time zero show intense fluorescence from ZP1 binding of zinc within glomeruli. b) The signal is reduced 5 min after application of 30 μ M TPA. c) Most of the signal is eliminated 10 min after TPA. A quantitative group analysis (ImageJ) of the change in the signal over the 10-min incubation with TPA is shown in panel (d). Signal intensities have been background subtracted and normalized (n=3). A statistical difference between time zero and 5 min ($p < 0.01$) and 10 min ($p < 0.0001$) time points is indicated by the *. A statistical difference between the 5 min and 10 min time points ($p < 0.01$) is indicated by the #.

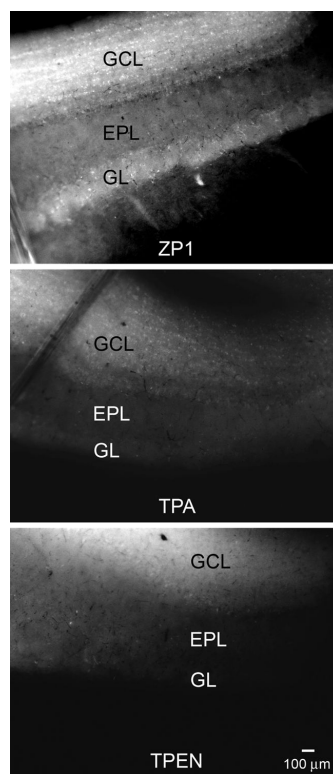


Figure 3. Chelation of zinc with TPA and TPEN produce similar results. Top panel: OB slice after incubation with 30 μ M ZP1 for 30 min. Middle panel: Chelation of zinc by incubation with 30 μ M TPA for 20 min substantially reduces the signal from ZP1. Bottom panel: The reduction in the ZP1 signal after zinc chelation with 30 μ M TPEN for 20 min was similar to the reduction seen with TPA.

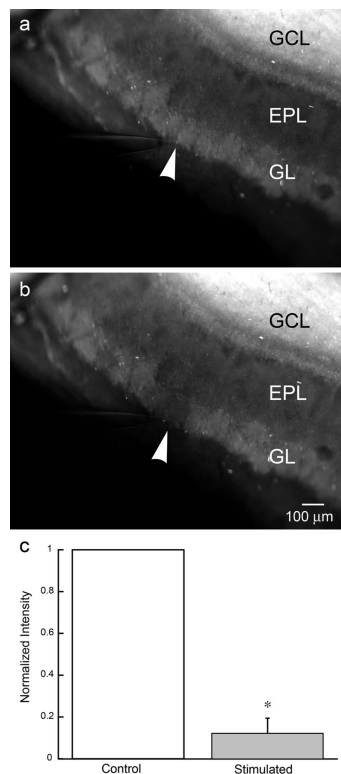


Figure 4.

Evoked release of glomerular zinc with patterned electrical stimulation. a) OB slices incubated in 30 μ M ZP1 for 30 min reveal a laminar distribution of vesicular zinc. The stimulating electrode is in place prior to stimulation. b) A pattern of electrical stimuli, designed to mimic the breathing cycle (five bursts, three pulses at 100 Hz separated by 250 ms) and delivered to the olfactory nerve layer for 10 min, evoked release of zinc from glomeruli adjacent to the stimulating electrode. c) A quantitative group analysis (ImageJ), of the background subtracted and normalized zinc fluorescence before and after electrical stimulation, shows the reduction in the zinc signal evoked by electrical stimulation (n=3). A statistical difference between the control and the stimulated signal intensity ($p < 0.002$) is indicated by the *. The position of the tip of the stimulating electrode in (a) and (b) is indicated by the white arrowhead. GCL (granule cell layer); EPL (external plexiform layer); GL (glomerular layer).

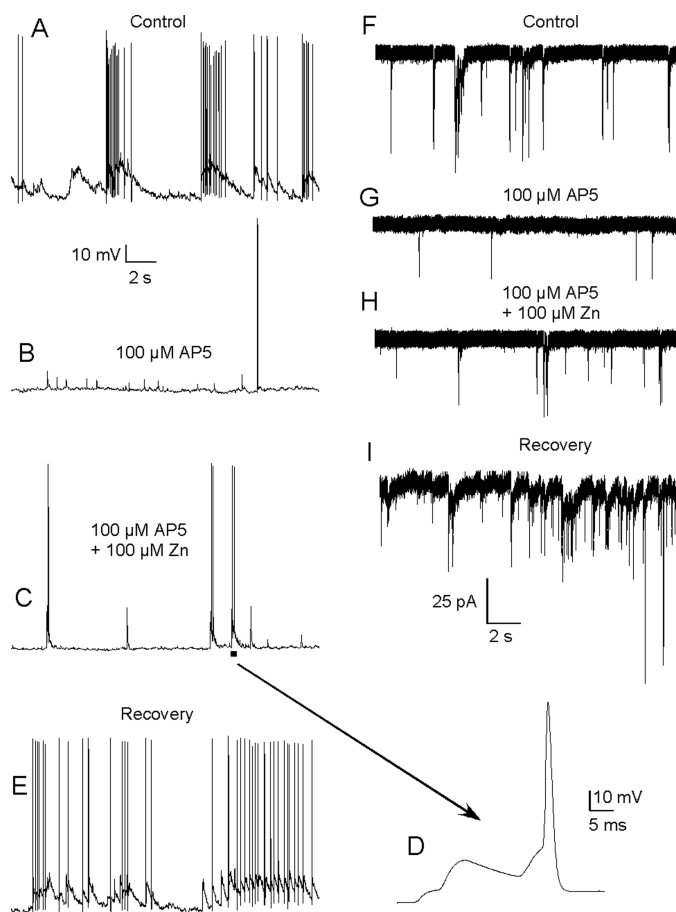


Figure 5. Extracellular zinc enhances AMPA receptor-mediated synaptic transmission. a) Glutamate-mediated excitatory synaptic events evoke EPSPs resulting in bursts of action potentials. b) Blockade of NMDA receptors, with the application of 100 μ M AP5, dramatically reduced excitation and isolated synaptic events mediated by AMPA receptors. c) Extracellular application of ZnCl₂ (100 μ M) enhanced the amplitude of AMPA receptor-mediated synaptic events. d) An expanded time scale of a segment of the trace in c) demonstrates how such potentiation increases the opportunity for synaptic summation and action potential generation. e) The effects of AP5 and Zn are rapidly reversible. f–i) To eliminate potential contributions of Zn on voltage-gated ion channels, the protocol shown in a–d) was reapplied in voltage-clamp mode. Zn also potentiated AMPA receptor-mediated EPSCs.